Reciprocal Inhibitory Connections and Network Synchrony in the Mammalian Thalamus

Molly M. Huntsman, Darrell M. Porcello, Gregg E. Homanics, Timothy M. DeLorey, John R. Huguenard*

Neuronal rhythmic activities within thalamocortical circuits range from partially synchronous oscillations during normal sleep to hypersynchrony associated with absence epilepsy. It has been proposed that recurrent inhibition within the thalamic reticular nucleus serves to reduce synchrony and thus prevents seizures. Inhibition and synchrony in slices from mice devoid of the γ-aminobutyric acid type-A (GABA$_A$) receptor β$_3$ subunit were examined, because in rodent thalamus, β$_3$ is largely restricted to reticular nucleus. In β$_3$ knockout mice, GABA$_A$-mediated inhibition was nearly abolished in reticular nucleus, but was unaffected in relay cells. In addition, oscillatory synchrony was dramatically intensified. Thus, recurrent inhibitory connections within reticular nucleus act as "desynchronizers."

Inhibitory circuits arising in the reticular thalamic nucleus (RTN) play important roles in various oscillatory activities related to sleep and some epilepsies (*1–5*). The major projections of inhibitory neurons in RTN are onto relay neurons in dorsal thalamus, but recurrent collaterals also provide intranuclear inhibition (*6*). It has been hypothesized that the latter connections regulate RTN inhibitory output during thalamic oscillations and prevent the hypersynchrony of generalized absence epilepsy (*7–9*). Inhibitory postsynaptic currents (IPSCs) in RTN neurons are mediated by the major inhibitory neurotransmitter, γ-aminobutyric acid, through GABA type A receptors. IPSCs in RTN differ from those in relay neurons (*10*), presumably due to differences in GABA$_A$ receptor subunit composition (*11*), which ultimately affect ligand affinity, channel gating, and modulation (*12*). In rodent thalamus, β$_3$ is one of a limited number of GABA$_A$ subunit mRNAs expressed in RTN and is absent from relay nuclei (*11*). Despite a lack of widespread gene expression in the adult rodent brain, β$_3$ knockout mice (β$_3^{-/-}$) exhibit many neurological impairments and are considered a model of Angelman's syndrome in humans

(*13*). We examined inhibitory function in thalamic slices of β$_3$ knockout mice to test whether elimination of this subunit would suppress intra-RTN inhibition and thus promote intrathalamic synchrony (*14*).

Voltage clamp recordings (*15*) were performed in the presence of GABA$_B$ and ionotropic glutamatergic blockers to specifically

isolate GABA$_A$ receptor–mediated IPSCs (*10, 16*). Spontaneous IPSCs (sIPSCs) in RTN neurons from controls were long lasting, with an average weighted decay time constant ($τ_{D,W}$) of 74.7 ± 5.9 ms (n = 19; Fig. 1, C and D). Infrequent sIPSCs were observed in RTN neurons of β$_3$ knockout mice and were much smaller and more brief than in wild-type (β$_3^{+/+}$) littermates. sIPSC decay was almost three times faster ($τ_{D,W}$ = 27.4 ± 2.4 ms, n = 26, P < 0.0001) in knockouts, whereas sIPSC amplitude and frequency in RTN were reduced by more than 50% (P < 0.0001; Fig. 1, A through D). Overall inhibitory efficacy was estimated by integrating total sIPSC charge per 1-s interval. In controls, the total charge was 3840 ± 1130 pC/s (n = 19), compared to a much reduced value of 130 ± 20 pC/s (n = 26, P < 0.0005) in β$_3$ knockouts. By contrast, excitatory connections were intact in RTN neurons of knockout mice. Spontaneous excitatory postsynaptic currents (sEPSCs) were comparable in amplitude (11 versus 14 pA in β$_3^{+/+}$ and β$_3^{-/-}$, respectively), half-width (1.1 versus 1.2 ms), and frequency (2.1 versus 3.0 Hz, n = 7 each).

Inhibition in thalamic relay neurons of the ventrobasal (VB) complex was unchanged in β$_3$ knockout mice—sIPSC amplitudes, decay kinetics, and frequency were comparable in wild-type control and knockout mice (Fig. 1, E through H). As in rat (*10*), sIPSC decay was faster in VB neurons (Fig. 1G) than in

Fig. 1. sIPSCs in RTN and VB neurons from wild-type (β$_3^{+/+}$) and knockout (β$_3^{-/-}$) mice. (**A** and **B**) Continuous traces depicting sIPSCs in individual RTN neurons from β$_3^{+/+}$ and β$_3^{-/-}$ mice. Note reduced sIPSC amplitude and frequency in the β$_3^{-/-}$ RTN neuron. (**C**) Averaged sIPSCs from cells in (A) (n = 93 IPSCs) and (B) (n = 51) superimposed on same time scale to illustrate decreased peak amplitude and duration in β$_3^{-/-}$ RTN neurons. (**D**) Population data (mean ± SE) for RTN sIPSC properties in β$_3^{+/+}$ (n = 19 cells) and β$_3^{-/-}$ mice (n = 26). *** = P < 0.0001. (**E** and **F**) Continuous sIPSC traces of individual VB neurons from β$_3^{+/+}$ and β$_3^{-/-}$ mice. Scale is same as in (A) and (B). (**G**) Average sIPSCs in VB cells from (E) (n = 167 IPSCs) and (F) (n = 294). (**H**) Population data (mean ± SE) for VB sIPSC properties of β$_3^{+/+}$ (n = 9 cells) and β$_3^{-/-}$ (n = 11) mice.

M. M. Huntsman, D. M. Porcello, J. R. Huguenard, Department of Neurology and Neurological Sciences, Stanford University Medical Center, Stanford University, Stanford, CA 94305, USA. G. E. Homanics, Department of Anesthesiology/Critical Care Medicine, University of Pittsburgh School of Medicine, Pittsburgh, PA 15261, USA. T. M. DeLorey, Molecular Research Institute, 845 Page Mill Road, Palo Alto, CA 94304–1011, USA.

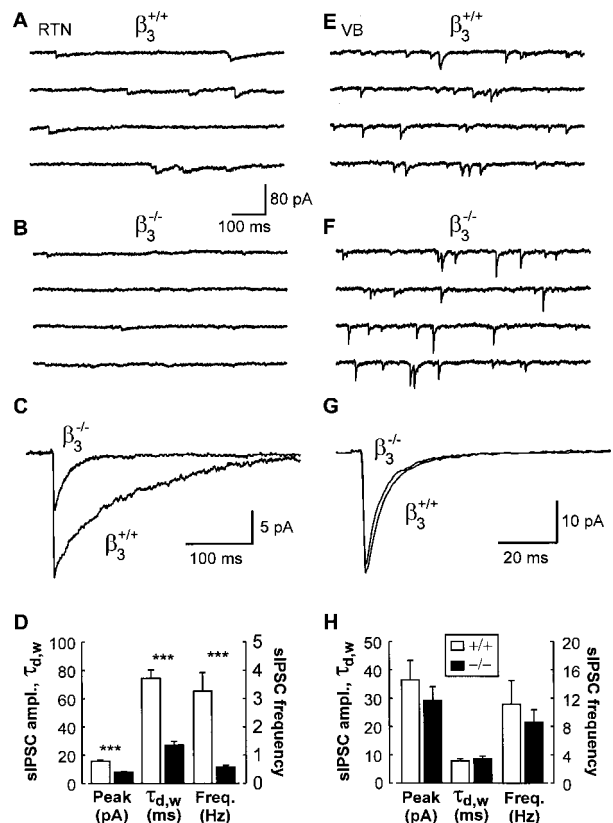*To whom correspondence should be addressed. E-mail: John.Huguenard@stanford.edu

RTN neurons (Fig. 1C).

To confirm the specific reduction in intra-RTN inhibition, we also assessed electrically evoked responses (17). Monosynaptic evoked IPSC (eIPSC) amplitudes in RTN neurons from β_3 knockout mice were reduced by about half in both amplitude and duration (Fig. 2). By contrast, eIPSCs in VB neurons of wild-type and knockout mice were indistinguishable in terms of amplitude (1.31 ± 0.33 nA, $n = 6$ versus 0.96 ± 0.28 nA, $n = 6$, $P > 0.4$) and duration ($\tau_{D,W}$ of 21.1 ± 3.4 ms versus 21.1 ± 2.5 ms, $P > 0.9$).

These data show that inhibitory efficacy is specifically reduced for the recurrent connections between RTN neurons of β_3 knockout mice, thus rendering part of the thalamic circuit defective. The thalamic network responsible for generating sleep and epilepsy-related oscillatory activity requires intact excitatory and inhibitory connections between RTN and relay cells (3–5). These connections appear to be normal in β_3 knockout mice as judged by the aforementioned properties of EPSCs in RTN cells and IPSCs in relay neurons. These mice then provided a unique opportunity to directly test for the functional role of RTN inhibitory collaterals (4, 7). Oscillatory activity was evoked by stimulation of the internal capsule in vitro (18) and, as previously shown (5), was GABA$_A$ receptor–dependent. In control slices, oscillatory responses were characterized by an initial fixed-latency burst (asterisks; Fig. 3A, left), followed by two to six repetitive bursts with variable latencies (arrowheads; Fig. 3A, left). In contrast, highly synchronous activity (for example, Fig. 3A, right) was obtained in the majority of slices (39 of 48, ~81%) from β_3

knockouts. Similar synchrony was rarely observed in wild-type slices (4 of 33, ~12%; $P < 0.0001$, Fisher's Exact Test). Interestingly, synchronous oscillations occurred spontaneously in a few knockout slices. The timing of burst occurrence was particularly notable in the knockouts—oscillations were both highly synchronous and phase-locked throughout their duration (diamonds; Fig. 3A, right).

Autocorellograms derived from control slices typically had distinctive large central peaks with much smaller and irregular satellite peaks (arrowheads; Fig. 3B, left). In contrast, autocorrelograms from knockout mice showed numerous satellite peaks of gradually decaying amplitude, with a less distinct central peak (Fig. 3B, right). In control slices, 29 ± 6% ($n = 9$) of the neuronal activity in RTN was deemed oscillatory (19), compared to 70 ± 6% ($n = 11$, $P < 0.001$) in β_3 knockout slices (Fig. 3C). Comparable oscillatory indices were obtained from VB recordings ($\beta_3^{+/+}$, 27 ± 4%, $n = 10$ versus $\beta_3^{-/-}$, 59 ± 5%, $n = 12$; $P < 0.001$). Therefore, knockout of β_3 resulted in highly synchronous and oscillatory activity throughout the RTN-VB network. Further support for synchrony was indicated by large-amplitude maximal extracellular field potentials ($\beta_3^{-/-}$, 86 ± 7.7 μV, $n = 36$ versus $\beta_3^{+/+}$, 13.6 ± 2.9 μV, $n = 30$; $P < 0.0001$), suggesting that local groups of neurons fire nearly simultaneously during the oscillatory response. Not only was local synchrony high, but oscillatory activity throughout the slice was tightly phase-locked. Cross-correlation analysis of dual recordings in VB complex demonstrated that phase differences in the knockouts were negligible (<4 ms) at distances of up to 500 μm (Fig. 3D). In contrast, oscillatory activity in control slices was characterized by phase lags that increased linearly with distance up to ~70 ms at 500 μm separation (Fig. 3D).

These results demonstrate that GABA$_A$ receptor–mediated IPSCs in RTN are impaired in β_3 knockouts. The resulting reduced inhibitory efficacy between RTN neurons thus leads to hypersynchrony that is detrimental to the normal function of the thalamic circuit. Consistent with this hypothesis, local application of GABA$_A$ antagonists within RTN of wild-type mouse slices enhanced oscillatory activity (20), in accordance with results previously reported in rat (7). These results indicate that reduced
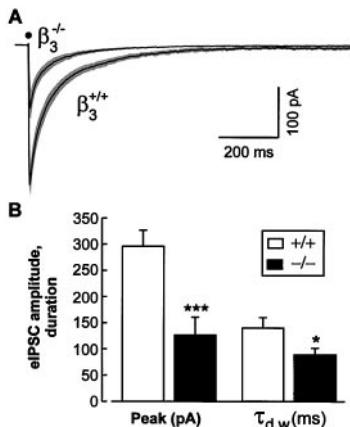
Fig. 2. Properties of monosynaptic eIPSCs recorded in RTN neurons. (**A**) Averages of eIPSCs evoked in individual RTN neurons of $\beta_3^{+/+}$ ($n = 5$ neurons) and $\beta_3^{-/-}$ ($n = 7$) mice as indicated. The shaded area flanking the averaged eIPSC represents the mean ± one standard error; ● = onset of stimulus. (**B**) Histogram of mean peak eIPSC amplitude and $\tau_{D,W}$ in $\beta_3^{+/+}$ and $\beta_3^{-/-}$ mice; *** = $P < 0.001$, * = $P < 0.05$.

Fig. 3. Simultaneous multi-unit recordings in VB and RTN during evoked oscillatory activity in acute thalamic slices in $\beta_3^{+/+}$ and $\beta_3^{-/-}$ mice. (**A**) Consecutive raw traces of thalamic oscillations in $\beta_3^{+/+}$ slices reveal repetitive burst activity (asterisks, arrows) at variable latencies (left panel; note considerable trial-to-trial variability). In contrast, highly synchronous, phase-locked oscillations were obtained in $\beta_3^{-/-}$ mouse slices (right panel; little trial-to-trial variability); ● = onset of stimulus. Vertical bars and diamonds represent fixed intervals of 121 ms. (**B**) Autocorrelograms of thalamic oscillations represented in (A). Note the small oscillatory components adjacent to the central peak in $\beta_3^{+/+}$ mice (arrowheads indicate satellite peaks) versus the multiple large peaks in $\beta_3^{-/-}$ mice. (**C**) Histogram of the oscillatory index computed from autocorrelograms from slices of $\beta_3^{+/+}$ and $\beta_3^{-/-}$ mice, *** = $P < 0.001$. (**D**) Phase difference in VB as a function of distance during oscillations generated in slices from $\beta_3^{+/+}$ and $\beta_3^{-/-}$ mice; □ = $\beta_3^{+/+}$, ■ = $\beta_3^{-/-}$, *** = $P < 0.001$, * = $P < 0.05$, n = two to seven slices for each point.
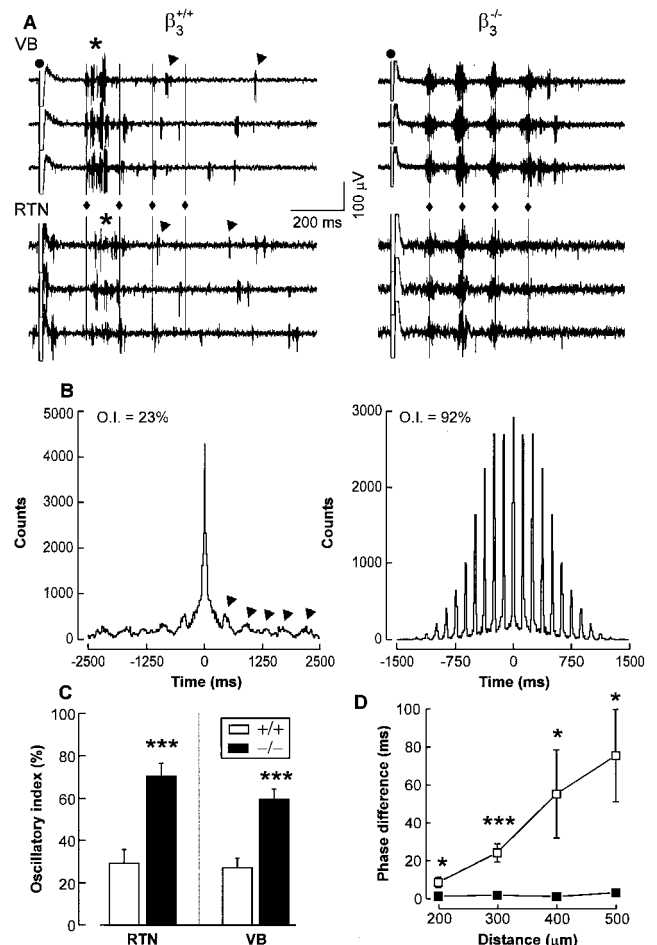
intra-RTN inhibition is sufficient to produce thalamic hypersynchrony.

The powerful effects of β₃ ablation could be explained by the dependence of GABA$_A$ responses in RTN neurons on relatively few receptor isoforms (*11*). GABA$_A$ receptor function is less impaired in hippocampal neurons of β$_3$ knockouts (*21*), which may reflect a lower dependence on this β subunit (*11*). The shortening of IPSC duration in β$_3$ knockouts potentially relates IPSC properties to neural circuit activity in the thalamus and may show how the specific functional deletion of intra-RTN connections affects phasic oscillations (*7, 8*). The role of intra-RTN connections in thalamic oscillations is controversial. These connections might either facilitate (*22*) or dampen oscillations (*7, 9, 23*). Our results, showing highly synchronous oscillations in animals lacking functional GABA$_A$ receptors in RTN, indicate that intra-RTN inhibition desynchronizes thalamic activity. Further, these data show how inactivation of a postsynaptic receptor gene can result in functional deletion of a specific neuroanatomical circuit and provide information regarding mechanisms of human disease (*13*).

References and Notes

1. M. Steriade and R. R. Llinas, *Physiol. Rev.* **68**, 649 (1988).
2. M. Steriade, D. A. McCormick, T. J. Sejnowski, *Science* **262**, 679 (1993).
3. J. R. Huguenard and D. A. Prince, *J. Neurosci.* **14**, 5485 (1994).
4. M. von Krosigk, T. Bal, D. A. McCormick, *Science* **261**, 361 (1993).
5. R. W. Warren, A. Agmon, E. G. Jones, *J. Neurophysiol.* **72**, 1993 (1994).
6. E. E. Scheibel and A. B. Scheibel, *Brain Res.* **1**, 43 (1966); E. G. Jones, *J. Comp. Neurol.* **162**, 285 (1975); C. L. Cox, J. R. Huguenard, D. A. Prince, *ibid.* **366**, 416 (1996); D. Pinault, Y. Smith, M. Deschênes, *J. Neurosci.* **17**, 3215 (1997).
7. J. R. Huguenard and D. A. Prince, *J. Neurophysiol.* **71**, 2576 (1994).
8. U. Kim, M. V. Sanchez-Vives, D. A. McCormick, *Science* **278**, 130 (1997).
9. M. V. Sanchez-Vives, T. Bal, D. A. McCormick, *J. Neurosci.* **17**, 8894 (1997).
10. S. J. Zhang, J. R. Huguenard, D. A. Prince, *J. Neurophysiol.* **78**, 2280 (1997).
11. W. Wisden, D. J. Laurie, H. Monyer, P. H. Seeburg, *J. Neurosci.* **12**, 1040 (1992). Peak expression levels of β$_3$ subunit are in hippocampus, cerebellum, pyriform cortex, and olfactory bulb. In thalamus, β$_3$ is restricted to RTN and midline nuclei.
12. R. L. Macdonald and R. W. Olsen, *Annu. Rev. Neurosci.* **17**, 569 (1994).
13. G. E. Homanics *et al.*, *Proc. Natl. Acad. Sci. U.S.A.* **94**, 4143 (1997); T. M. DeLorey *et al.*, *J. Neurosci.* **18**, 8505 (1998).
14. Electroencephalographic oscillations during sleep and absence epilepsy result from synchronous activity in the cerebral cortex. They depend on synaptic interactions among neurons of RTN, thalamocortical relay nuclei, and cerebral cortex [reviewed in (*2*)].
15. Experiments were performed in accordance with procedures established by the Administrative Panel on Laboratory Animal Care at Stanford University. Briefly, adult mice, ranging in age from postnatal day 21 (P21) through P94 were anesthetized with pentobarbital (55 mg/kg body weight). We obtained 200-μm horizontal slices, using chilled slicing solution [115 mM choline-chloride, 26 mM NaHCO$_3$, 10 mM glucose, 2.5 mM KCl, 1.25 mM NaH$_2$PO$_4$, 10 mM MgSO$_4$, and 0.5 mM CaCl$_2$ (290 mosm)], and then incubated the slices at 32C in physiological saline (2 mM CaCl$_2$, 2 mM MgSO$_4$, and 126 mM NaCl) for 1 hour. Recordings (L/M-EPC7, Darmstadt, Germany) were at room temperature (21° to 23°C) with perfusion of physiological saline (2 ml/min). The holding potential was −60 mV, and with E$_{Cl}$ ≈ 0 mV, IPSCs were inward events. RTN and VB neurons were identified and recorded in a chamber affixed to the stage of an upright microscope (Leitz Laborlux). Electrodes were filled with pipette solution [135 mM CsCl, 5 mM QX314, 2 mM MgCl$_2$, 10 mM EGTA, 10 mM Hepes (pH 7.3)] and had resistances of 2.0 to 3.3 megohms. IPSCs were filtered at 1 kHz and stored on VCR tape (Neuro-corder, Cygnus Technology, Delaware Water Gap, PA). Spontaneous events were digitized with Axotape, version 2 (Axon Instruments), then were sorted and analyzed using Detector (version 4.8, J. R. Huguenard), Scan (J. R. Dempster), and Metatape (version 14.0, J. R. Huguenard). Unless otherwise noted, all statistical values indicate results of Student's *t* test.
16. Iontotropic glutamate receptors were blocked via bath application of 6,7-dinitroquinoxaline-2,3-dione (20 μM DNQX) [Research Biochemicals International (RBI), Natick, MA] and (+/−)-2-amino-5-phosphono-pentanoic acid (100 μM AP-5) (RBI). Inhibitory GABA$_B$ receptors were blocked with CsCl and QX-314 (5 mM) in the internal pipette solution. IPSC decay was quantified by fitting double exponentials to averaged sIPSCs (>50 events from each neuron). Weighted decay time constants (τ$_{D,W}$), derived from these fitted curves, provide a simple means to quantify IPSC duration [M. V. Jones and G. L. Westbrook, *J. Neurosci.* **17**, 7626 (1997)].
17. eIPSCs were obtained by stimulating RTN with a bipolar tungsten electrode. Stimuli were 1.5 times threshold (1.5 to 4 mA; 80 to 200 μs).
18. Extracellular multiunit recordings were performed as previously described using tungsten electrodes placed in RTN and the VB complex [D. Ulrich and J. R. Huguenard, *Neuron* **15**, 909 (1995)]. Extracellular stimulus (20 to 60 V, 30 μs, 0.05 Hz) to the internal capsule evoked oscillatory responses. Signals were band-pass filtered (30 Hz to 3 kHz) and recorded at 10 kHz, using Axotape, version 2.0 (Axon Instruments, Foster City, CA). Field responses were filtered between 3 and 100 Hz. Oscillations were blocked by 10 μM bicuculline methiodide (BMI) or 50 μM picrotoxin.
19. P. König, *J. Neurosci. Methods* **54**, 31 (1994). A modified Gabor function measured distinct autocorrelogram components: a central peak (CP), an exponentially decaying cosine function (Osc), and an offset (Off). Oscillatory index was then Osc/(CP + Osc + Off) × 100%.
20. BMI (*n* = 18 slices) or picrotoxin (*n* = 4) enhanced oscillatory output when applied locally (500 μM via pressure application pipette) to RTN (137 ± 13% of control, *P* < 0.0001), but not VB (13 ± 2% of control, *P* < 0.01).
21. M. D. Krasowki, C. E. Rick, N. L. Harrison, L. L. Firestone, G. E. Homanics, *Neurosci. Lett.* **240**, 81 (1998).
22. M. Steriade, L. Domich, G. Oakson, M. Deschênes, *J. Neurophysiol.* **57**, 260 (1987); A. Destexhe, D. Contreras, T. J. Sejnowski, M. Steriade, *ibid.* **72**, 803 (1994).
23. G. Ahlsén and S. Lindström, *Brain Res.* **236**, 482 (1982); D. Ulrich and J. R. Huguenard, *J. Neurophysiol.* **78**, 1748 (1997).
24. We thank C. Ferguson and J. Steinmiller for technical assistance and L. L. Firestone, R. W. Olsen, P. S. Buckmaster, N. A. Lambert, and D. A. Prince for support, encouragement, and helpful comments. Supported by NIH grants NS06477, NS34774, AA10422, and GM52035; the Pimley Research Fund; and the University Anesthesiology and Critical Care Medicine Foundation. Additional information may be obtained at http://tonto.stanford.edu/~john.

Prevention of Constitutive TNF Receptor 1 Signaling by Silencer of Death Domains

Yingping Jiang, John D. Woronicz, Wei Liu, David V. Goeddel*

Tumor necrosis factor receptor type 1 (TNF-R1) contains a cytoplasmic death domain that is required for the signaling of TNF activities such as apoptosis and nuclear factor kappa B (NF-κB) activation. Normally, these signals are generated only after TNF-induced receptor aggregation. However, TNF-R1 self-associates and signals independently of ligand when overexpressed. This apparent paradox may be explained by silencer of death domains (SODD), a widely expressed ~60-kilodalton protein that was found to be associated with the death domain of TNF-R1. TNF treatment released SODD from TNF-R1, permitting the recruitment of proteins such as TRADD and TRAF2 to the active TNF-R1 signaling complex. SODD also interacted with death receptor–3 (DR3), another member of the TNF receptor superfamily. Thus, SODD association may be representative of a general mechanism for preventing spontaneous signaling by death domain–containing receptors.

TNF is a pleiotropic cytokine that signals through two distinct TNF receptors belonging to the rapidly expanding TNF receptor superfamily. Many of TNF's best characterized

Tularik, Two Corporate Drive, South San Francisco, CA 94080, USA.

*To whom correspondence should be addressed. E-mail: goeddel@tularik.com

signaling pathways, such as induction of apoptosis and activation of the transcription factor NF-κB, are initiated by TNF-R1, whereas TNF-R2 appears to play a direct role in only a limited number of TNF responses (*1*). The intracellular portion of TNF-R1 contains a "death domain" of about 70 amino acids that is required for the signaling of apoptosis and NF-κB activation (*2, 3*). Many